

Interstellar neutral oxygen in a two-shock heliosphere

V. Izmodenov¹, Yu.G. Malama², and R. Lallement³

¹ Moscow State University, Department of Mechanics and Mathematics, Aeromechanic division, Moscow 199899, Russia

² Institute for Problems in Mechanics, Russian Academy of Sciences, Prospect Vernadskogo 101, Moskow 117526, Russia

³ Service d'Aéronomie du CNRS, BP 3, F-91371 Verrieres-le-Buisson, France

Received 10 January 1996 / Accepted 14 May 1996

Abstract. A fraction of the interstellar neutral atoms crosses the interface between the solar wind and the ionized component of the local interstellar medium, and enters the heliosphere. The number of penetrating atoms depends on both the interface structure and the strength of the atom-plasma interaction, i.e. on the atom type.

In this paper we consider the penetration of the interstellar oxygen. Oxygen atoms are of particular interest, because they are strongly coupled with the protons through charge exchange reactions, and because they are now observed under the form of pick-up ions and anomalous cosmic rays, providing new observational tests of the processes at work at the boundary of the heliosphere. Our calculations are based on the Baranov two-shock heliospheric model (Baranov and Malama, 1993). Oxygen number density distributions are computed through a Monte-Carlo simulation of the O and O⁺ flows through the H and H⁺ interface. The model accounts for direct charge-exchange (O atoms with protons), reverse charge-exchange (O ions with neutral H), photoionization and solar gravitation. Source distributions of O⁺ pick-up ions resulting from oxygen atom ionization are also produced, as well as density distributions of the oxygen ions in the heliosphere, assuming that newly created oxygen ions are instantaneously assimilated to the plasma. In the light of these results we compare the recent measurements of pick-up oxygen ions with the Local Interstellar Cloud oxygen abundance deduced from nearby star spectroscopy. The comparison shows that the measurements do not preclude, and even suggest, a significant ionization of the ambient interstellar medium.

Key words: Interplanetary medium – ISM: general – atomic processes – solar neighbourhood

1. Introduction

Our solar system is moving through a partially ionized interstellar medium. The ionized fraction of this local interstellar

medium (LISM), interacts with the expanding solar wind and forms the LISM - Solar Wind interface. The characterization of this interface is one of the major objectives for the near future in astrophysics and space plasmas physics. For recent reviews see Holzer (1989), Axford (1989), Suess (1990), Baranov (1990), Lee (1993), Jokipii and McDonald (1995). The choice of an adequate model of the interface depends on the parameters of the parcel of interstellar gas surrounding the Sun, also called the Local Interstellar Cloud (LIC). Some of these parameters, as the Sun/LISM relative velocity, or the LISM temperature are now well constrained (Witte et al, 1993, Lallement & Bertin, 1992, Linsky et al, 1993, Lallement et al, 1995), but unfortunately there are no direct ways to measure the local interstellar electron (or proton) density, nor the local interstellar magnetic field, while these two parameters govern the structure and the size of our heliosphere. Therefore, there is a need for indirect observations which can bring stringent constraints on the plasma density and the shape and size of the interface to allow for the choice of an adequate theoretical model. Such constraints should help to predict when the two Voyager spacecraft will cross the interface, and whether or not they will be able to perform and transmit direct observations.

Among the various types of diagnostics are the observations of species which can penetrate deeply in the heliosphere, as the interstellar neutral atoms. These neutrals suffer significant modifications during the crossing of the interface (Wallis, 1975; Holzer, 1989; Osterbart and Fahr, 1992; Malama, 1991; Gangopadhyay and Judge, 1989). These modifications depend on the structure of the interface and the penetration factor of the atoms through the interface. Models show that the changes in the abundances and velocity distributions due to the interface filtering do vary strongly from one species to the other, because they depend on the strength of the coupling between the atom and the ionized species. As a result, the relative abundances and the velocity distributions of the different species inside the heliosphere are different from the original interstellar abundances and velocity distributions. In fact there are two types of diagnostics in connection with the perturbations of the neutrals. First, species-to-species comparisons within the heliosphere are in some cases sufficient to quantify the amount

Send offprint requests to: R. Lallement

of perturbations at the interface. In particular, a long-standing debate has been the comparison between the properties of the heliospheric neutral helium and those of the heliospheric neutral hydrogen. In principle neutral helium velocity and temperature are identical to those in the original LISM due to the extremely weak neutral/plasma coupling. In this respect, analyses of the backscattered radiation in the resonance line of H I $\lambda 1216$ and He I $\lambda 584$, together with models of the penetration of interstellar neutrals into interplanetary space, have brought useful information on the neutral component of the LISM and have allowed an indirect detection of the terminal shock by showing evidence for a neutral H deceleration (Lallement et al, 1993).

The second method is the comparison between the local interstellar medium properties, which can be derived e.g. from nearby stars spectroscopy, and the properties of the interstellar species inside the heliosphere. Not only the neutrals themselves but also the two types of derivatives of the neutrals, the pick-up ions and the anomalous component of cosmic rays (ACR), can be used to constrain the perturbations at the interface. As a matter of fact, according to the now well established ACR theory (Jokipii J.R., 1971; Fisk L.A., Kozlovsky B., Ramaty R., 1974, Pesses et al, 1981, Cummings et al, 1984) the sources of the ACR are the LISM atoms which penetrate in the heliosphere where they get ionized. The resulting ions are convected with the plasma as pick-up ions towards the termination shock where they are accelerated to high energies by Fermi acceleration and the ACR are this fraction of the pick-up ions which, after outwards convection by the solar wind, has been accelerated. Pick-up ions have been observed close to the Sun (e.g. Mobius et al, 1988, Gloeckler et al, 1995) and ACR in the whole heliosphere with in particular the two Voyager (e.g. Cummings and Stone, 1990). Observations of both types of ions can potentially bring extremely important constraints on the relative abundances of the heliospheric neutral atoms (Fahr, 1991, Fahr et al, 1995, Frisch, 1995) just after their entrance in the heliosphere. These results can then be compared with LISM abundances, and, through reliable models predicting the filtration of the different species as a function of the interface parameters, a self-consistent picture should be buildt.

The major difficulty when modelling the coupling between heliospheric interstellar neutrals and the plasmas is related to the fact that, at variance with charged particles, neutral atoms have an interaction length as large as the characteristic length of the interface, and penetrate deeply into the heliosphere. A significant amount of work has been done on the heliospheric interface filtering of hydrogen (Wallis, 1975; Baranov et al., 1979; Ripken and Fahr, 1983; Fahr and Ripken, 1984; Bleszynski, 1987; Gangopadhyay and Judge 1989, Baranov et. al., 1991, Osterbart & Fahr, 1992; Baranov & Malama 1993), and both hydrogen and helium (Bleszynski, 1987), primarily motivated by their large cosmic abundances and the availability of observations of resonantly scattered solar radiation by H and He atoms having penetrated the heliosphere.

There has been more recently an increasing interest in heavier elements of the LISM, in particular O, N, Ne, C and others. This was initially due to experimental projects devoted to the

detection of the backscattered radiation in the resonance lines of these elements. In particular, solar radiation scattered by the oxygen particles could be measured in the far UV at the 1304.Å primary resonance line (Bowyer & Fahr, 1989; Fahr, 1989; Fahr et. al. 1995 and references therein). However, this interest in minor species is now growing due to the recent successful detections of pick-up (Geiss et al, 1994) and ACR (Cummings et al, 1990) ions, with the Ulysses and Voyager spacecraft respectively. Oxygen is of particular interest, because it is one of the most perturbed elements due to its large charge exchange cross-section with the protons. Its entrance in the heliosphere has thus been thought to be a very good diagnostic of the interstellar plasma density (e.g. Fahr 1991). Initial calculations suggested a very small filtration factor, even for a very low interstellar plasma density. Here we call the filtration factor the ratio between the neutral oxygen density inside the heliosphere, at a large enough distance from the Sun for the direct solar wind and EUV ionization to be insignificant, and the initial interstellar neutral oxygen density outside the heliosphere, in the unperturbed interstellar medium. The filtration factor is a measurement of the coupling with the plasma, and then of the interstellar plasma density. According to these first results, the quasi-normal heliospheric oxygen abundance inferred from the ACR, implying a very large filtration factor, was incompatible with a non negligible LISM plasma density. Contrary to these previous calculations (Fahr, 1991), an improved modelling has shown that the degree of penetration is not so low, at least in the case of a Parker's type interface and a modified twin-shocks model with incompressible plasma and no gravitation (Fahr et al, 1995). Recently Frisch (1994) has demonstrated how oxygen measurements could be used in conjunction with carbon data to infer the interstellar electron density in the LISM. However, filtration of neutral oxygen and neutral carbon at the interface should be taken into account to obtain a more precise result.

In the present paper, we discuss the penetration of the neutral oxygen, whose cosmic LISM abundance is third, inside the heliosphere, through a realistic two shocks interface. The model allows for plasma compressibility, and includes gravitation. The large cross-section for charge-exchange with the protons, comparable to the neutral H cross-section, implies that the structure of the plasma interface has a strong influence on the characteristics of the oxygen atoms into heliosphere. However, there is an important difference between the two species. In the case of neutral hydrogen (charge-exchange $H + H^+ \rightarrow H^+ + H$), its abundance makes the quantity of newly created H and H^+ large enough to influence the overall structure of the interface (Baranov and Malama, 1993). For oxygen, its small cosmic abundance makes the newly created species unimportant, and it is possible to neglect the effect of charge-exchange on the H and H^+ parameters. It has to be noticed that neglecting the counter-back reaction onto the hydrogen and protons does not mean that the charge-exchange inverse reaction (O^+ with H) is negligible in comparison with the direct charge-exchange (O with H^+), something assumed in the past (Fahr and Ripken, 1984). As far as we are concerned with oxygen distribution, both reactions

are equally important. The inverse process has been taken into account recently for the first time by Fahr & al (1995).

The basic principles for the present theoretical description (gas dynamics for the plasma, kinetic approach for the neutrals) can be found in Malama (1991). Instead of the solution of the Boltzmann integro-differential equation calculated by Osterbart & Fahr (1992) and Fahr & al (1995), the present calculation is based on a Monte - Carlo simulation of the flow of O and O⁺ through the H and H⁺ interface (Bleszynski, 1987; Gangopadhyay & Judge 1989; Malama, 1991; Baranov & Malama, 1993). It uses the Baranov two-shock interface model which is a self-consistent gasdynamic model of the solar wind interaction with the local interstellar medium, which takes into account the mutual influence of the plasma component of the LISM and the LISM H atoms in the approximation of axial symmetry (Baranov and Malama, 1993). The oxygen and oxygen ions simulation is started in such an already self-consistent H atoms and protons background.

Such a modelling of the neutral oxygen flow through the interface provides the production term for the pick-up ions, of direct relevance to pick-up and anomalous cosmic rays measurements. More precisely, it provides the number and the location of newly created oxygen ions in heliosphere due to ionization and charge-exchange processes, the density distribution of the pick-up ions, assuming new born ions are picked up by the plasma instantaneously, and subsequently the source term for the acceleration processes. Ideally, such a model applied to pick-up and ACR data should provide heliospheric interstellar abundances on one hand, which can be compared with original interstellar abundances on the other. Because, independently, the ACR spectral and spatial gradients observations by the outer probes constrain the shock location (and then the structure of the interface) through diffusion- convection-acceleration models (Cummings et al, 1993), then, if the interstellar plasma pressure is the dominant confining agent for the heliosphere, a self consistency check of this pressure (or of the plasma density) should be obtained in the future from the two types of modelling. Simultaneously, the heliospheric radio emissions detected by the Voyager, which depend on the interstellar plasma density too (Kurth and Gurnett, 1993), have to be found compatible with the other descriptions.

The core of this paper is divided into five sections. In Sect. 2 is recalled the basic structure of the Baranov and Malama (1993) LISM vs solar wind interaction region, which is the starting point for the oxygen flow simulation. Sect. 3 describes the mathematical formulation of the problem, while Sect. 4 describes the computational method. In the fifth section results are presented for both neutral and pick-up ions. In Sect. 6 we discuss further the particular importance of the oxygen penetration in relation with the observations.

2. Self-consistent two-shock model of the LISM-solar wind interaction

In this paper we start with the self-consistent "supersonic" interface model computed by Baranov and Malama (1993). It is

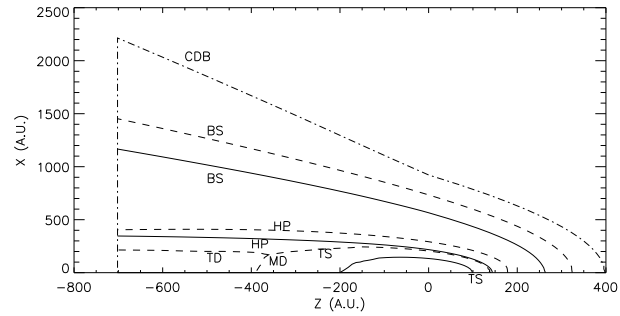


Fig. 1. The LISM-solar wind interaction scheme and the computed boundary surfaces according to the two-shocks model of Baranov & Malama (1993). The solid lines are the results for case b) (plasmas plus neutrals) and the dash lines for case a) (pure plasma-plasma interface). The positions of the bow shock (BS), the solar wind terminal shock (TS), the heliopause (HP), the tangential discontinuity (TD), the Mach disc (MD) and the computation domain boundary (CDB) are indicated.

based on an iterative method combining a gas-dynamical model characterized by two shock waves, a solar wind termination shock (TS) and an interstellar bow shock (BS), and one contact discontinuity, the heliopause (HP) (see Fig. 1), with a Monte-Carlo simulation for the neutral H flow through the plasma field. This axisymmetric model assumes that the interstellar medium is three-fluid with neutral (H-atoms) and plasma (electrons and protons) components. The boundary conditions for the proton density, the bulk velocity and the Mach number of the solar wind at the Earth's orbit are taken as:

$$n_{p,E} = 7.00\text{cm}^{-3}, v_E = 450\text{km/s}, M_E = 10$$

The same quantities for the unperturbed interstellar medium are:

$$n_{p,\infty} = 0.10\text{cm}^{-3}, v_\infty = 26\text{km/s}, M_\infty = 1.91$$

The corresponding temperature in the LISM is 6700 K. The temperature and the velocity of the unperturbed interstellar flow are in agreement with the heliospheric neutral helium parameters derived by Witte et al (1993) and the LIC parameters deduced from ground-based and Space Telescope stellar spectra (Lallement and Bertin, 1992, Linsky et al, 1993).

The number density of H atoms in the unperturbed LISM is either

$$\text{a) } n_{H,\infty} = 0\text{cm}^{-3},$$

$$\text{or b) } n_{H,\infty} = 0.14\text{cm}^{-3}.$$

Case a) corresponds to the pure plasma-plasma interaction, because interstellar neutrals are absent. It does not correspond to the actual situation, which is better represented by case b). However, it is interesting to consider the case a) and the comparison between a) and b), for both the structure (and size) of the interface (fig. 1), and for the neutral oxygen filtering (see Sect. 4).

The computational domain is delimited by a sphere of radius $R_{\min} = 1\text{AU}$ as the inner boundary, and, as the outer boundary, by a surface whose section $R_{\max}(\theta)$ is the contour labelled CDB in Fig. 1 on the upwind side, and a surface $Z = \text{cste} = Z_{\min}$ on the

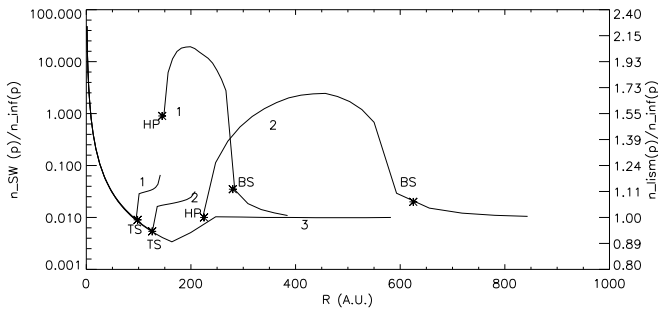


Fig. 2a. Densities of the solar wind and of the LISM's plasma component as functions of heliocentric distance. The location of the heliopause separates the left scale (for the solar wind parameters) and the right scale (for the parameters of the LISM's plasma component). Curve 1 corresponds to the upwind direction, curve 2 corresponds to the perpendicular direction to the running flow, (or sidewind direction) curve 3 corresponds to the downwind direction. Curve 3 should be read with the left scale. Positions of TS, HP, BS are shown by stars.

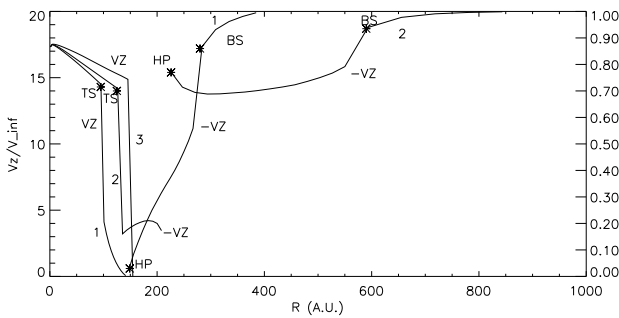


Fig. 2b. Z-component (along the wind axis) of the solar wind and the LISM's plasma component velocities as functions of heliocentric distance. The location of the heliopause separates the left scale (for solar wind parameters) and the right scale (for parameters of the LISM's plasma component). Curve 1 corresponds to the upwind direction, curve 2 corresponds to the perpendicular direction, curve 3 to the downwind direction. Curve 3 should be read with the left scale. The positions of TS, HP, BS are shown by stars.

downwind side. Here θ is the polar angle counted from the upwind axis. This outer boundary extends up to $R_{\max}(0)=400\text{AU}$ on the upwind side and up to $Z_{\min} = -700\text{AU}$ on the downwind side. The surface $R_{\max}(\theta)$ is chosen in such a way that the LISM perturbations outside the computational region are negligible. Fig. 1 shows the structure of the interface in the XOZ plane, where the OZ axis coincides with the axis of symmetry and is antiparallel to the velocity vector of the LISM's (the Sun is at the center of the coordinate system). In this figure, 'BS' is the bow shock formed in the LISM due to the deceleration of the plasma component. 'HP' is the heliopause (contact or tangential discontinuity) separating the LISM plasma compressed by the bow shock BS, from the solar wind compressed by the termination shock TS. Solid lines (resp. dashed lines) are for the case b (resp. a). Hydrogen atoms which penetrate the solar wind flow through the whole BS-HP-TS plasma structure. Shown in Fig. 2 are the proton and H density distributions, the bulk velocities and the temperatures issued from this model, which are

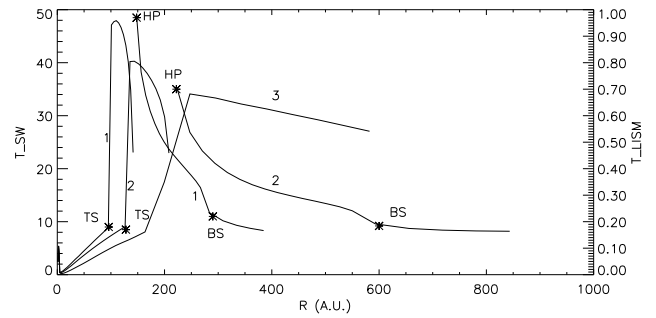


Fig. 2c. Temperature of the solar wind and the LISM's plasma component as functions of heliocentric distance in units of $m_H v_\infty^2/2$. The value 0.17 corresponds to the outer temperature of 6700K. The maximum value 48 corresponds to $1.90 \cdot 10^6$ K in the compressed solar wind region. The location of the heliopause separates the left scale (for solar wind parameters) and the right scale (for parameters of the LISM's plasma component). Curves 1,2,3 for upwind, sidewind and downwind respectively. Curve 3 corresponds to the left scale. The positions of TS, HP, BS are shown by stars.

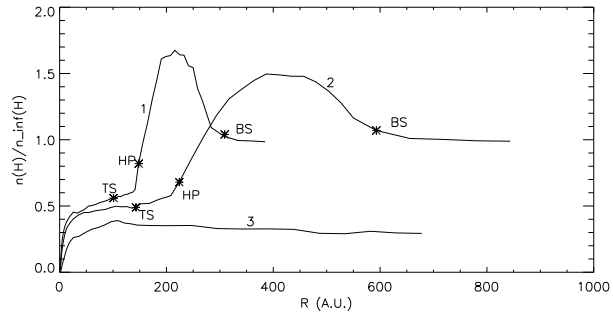


Fig. 2d. Neutral H atom density of LISM origin as a function of heliocentric distance r for the upwind direction (1), the sidewind or perpendicular direction (2) and the downwind direction (3). n_∞^H is the H atom number density in the unperturbed LISM. Positions of TS, HP and BS are shown by stars.

now used in the present study as background properties for the inflowing neutral oxygen. Fig. 2a displays the LISM protons density, Fig. 2b the proton velocity component parallel to the Z-axis, Fig. 2c the proton temperature, and Fig. 2d the number density of the neutral H atoms, for three directions: the upwind direction (Curve 1, $\theta = 0$), the "sidewind" or direction perpendicular to the flow axis (curve 2, $\theta = \frac{\pi}{2}$) and the downwind direction (curve 3, $\theta = \pi$). These distributions are discussed in details in Baranov & Malama (1993). Note that, at variance with a pure plasma/plasma interaction, the LISM, upstream from the bow shock, as well as the solar wind, upstream from the terminal shock, both have space-varying characteristics showing that they "feel" the shock before crossing it. This is due to resonance charge exchange processes with the neutrals and the 'pick-up' of the 'new' protons.

3. Formulation of the problem

We are interested here in the distribution of oxygen of interstellar origin in the computational domain shown in Fig. 1. The

flow of atoms must be described kinetically, because, as already said, the free path length of the neutral atoms is of the order of the size of the interaction region. In order to obtain the kinetic distribution function, Boltzman's equation must be solved:

$$\begin{aligned} \mathbf{w}_o \frac{\partial f_o(\mathbf{r}, \mathbf{w}_o)}{\partial \mathbf{r}} + \frac{F_g}{m_o} \frac{\partial f_o(\mathbf{r}, \mathbf{w}_o)}{\partial \mathbf{w}_o} = \\ -f_o(\mathbf{r}, \mathbf{w}_o) \int |\mathbf{w}_o - \mathbf{w}_p| \sigma_{ex}^{OH^+} f_p(\mathbf{r}, \mathbf{w}_p) d\mathbf{w}_p \\ + f_H(\mathbf{r}, \mathbf{w}_H) \int |\mathbf{w}_{o^+} - \mathbf{w}_H| \sigma_{ex}^{HO^+} f_{o^+}(\mathbf{r}, \mathbf{w}_{o^+}) d\mathbf{w}_{o^+} \\ - \beta_i f_o(\mathbf{r}, \mathbf{w}_o) \end{aligned} \quad (1)$$

where $f_o(\mathbf{r}, \mathbf{w}_o)$ is the oxygen atom distribution function, $f_p(\mathbf{r}, \mathbf{w}_p)$ the local Maxwell distribution function of the protons with the hydrodynamical values $\rho(\mathbf{r})$, $\mathbf{v}(\mathbf{r})$, $T(\mathbf{r})$ from the model described above; $f_H(\mathbf{r}, \mathbf{w}_H)$ is the hydrogen atom distribution function, $f_{o^+}(\mathbf{r}, \mathbf{w}_{o^+})$ the local Maxwell distribution function of oxygen ions with the hydrodynamic values described later, \mathbf{w}_o , \mathbf{w}_p , \mathbf{w}_{o^+} , \mathbf{w}_H the individual velocities of oxygen atoms, protons, oxygen ions and hydrogen atoms, $\sigma_{ex}^{OH^+}$ the charge exchange cross-section of an O-atom with a proton, $\sigma_{ex}^{HO^+}$ the charge exchange cross-section of an hydrogen atom with an oxygen ion, β_i the photoionization rate, m_o the mass of the oxygen atom, F_g the solar gravitational force.

Eq. (1) takes into account the following processes in which oxygen is involved:

a) the solar gravitation: the potential energy is $\Pi = \frac{G}{r}$, where $G = G^* m_O M_O$, G^* is the universal gravitational constant, and M_O - the mass of the Sun.

b) the charge exchange of O-atoms with protons: $O + H^+ \rightarrow O^+ + H$, with a charge exchange rate β_{ex} , given by formula: $\beta_{ex}(\mathbf{r}) = n_p \int u \sigma_{ex}^{OH^+}(u) f_p(\mathbf{r}, \mathbf{w}_p) d\mathbf{w}_p$ where $u = |\mathbf{w}_p - \mathbf{w}_o|$ is the relative atom-proton velocity, and $\sigma_{ex}^{OH^+} = (a_1 - a_2 \ln(u))^2 \text{ cm}^2$ is the charge exchange cross section. a_1 , a_2 are constants, $a_1 = 5.93 \times 10^{-8}$, $a_2 = 1.74 \times 10^{-9}$ (Stebbins & al, 1964, Banks & Kockarts, 1973). The relative velocity is measured in cm/s .

c) the reverse charge exchange of hydrogen atoms with oxygen ions: $O^+ + H \rightarrow H^+ + O$. The cross section for this reaction is connected with the cross section of the direct charge exchange by the following relation:

$$\sigma_{ex}^{HO^+} = \frac{9}{8} \sigma_{ex}^{OH^+} \text{ (Stebbins \& al, 1964)}$$

d) the photoionization: the rate is given by:

$$\beta_i^O = \beta_{pe}^O \left(\frac{r_e}{r} \right)^2, \beta_{pe}^O = 3.2 \times 10^{-7} \text{ sec}^{-1}$$

(Banks and Kockarts, 1973), where β_{pe}^O is the photoionization rate at the Earth's orbit and r_e - is 1 A.U.

Collisions between oxygen atoms and electrons are not taken into account in the present model. These collisions may be significant in the heliosheath where solar wind electrons are

hot, and may ionize substantially the oxygen. Following the arguments of Fahr, Osterbart and Rucinski (1995) and the Lotz (1967) formula, we have estimated this effect for an interstellar plasma density of 0.1 cm^{-3} . An upper limit of 9% extinction between the termination shock and the heliopause can be derived, assuming a 2.10^6 K temperature everywhere in the heliosheath. This upper limit is high enough to deserve further work, and we are considering the possibility of modifying the simulation to include it in the future.

Eq. (1) contains the oxygen ions distribution function $f_{o^+}(\mathbf{r}, \mathbf{w}_{o^+})$. This distribution function obeys a relation of the type:

$$\frac{df_{o^+}}{dt} = I(f_{O^+}, f_p, f_o, f_H) \quad (2)$$

which is expressed according to the plasma structure.

Actually, we do not calculate explicitly the distribution function $f_o(\mathbf{r}, \mathbf{w}_o)$, but its first moments, i.e. the number density of oxygen atoms $n_o(\mathbf{r})$, the bulk velocity $\mathbf{v}_o(\mathbf{r})$, the 'temperature' (average kinetic energy) $T_o(\mathbf{r})$, and the pick-up ions source term $q_1(\mathbf{r})$ defined by:

$$n_o(\mathbf{r}) = \int f_o(\mathbf{r}, \mathbf{w}_o) d\mathbf{w}_o$$

$$\mathbf{v}_o(\mathbf{r}) = \frac{\int \mathbf{w} f_o(\mathbf{r}, \mathbf{w}_o) d\mathbf{w}_o}{n_o(\mathbf{r})} \quad (3)$$

$$T(\mathbf{r}) = \frac{\int m_o (\mathbf{w} - \mathbf{v}(\mathbf{r}))^2 f_o(\mathbf{r}, \mathbf{w}_o) d\mathbf{w}_o}{2n_o(\mathbf{r})} \quad (4)$$

$$q_1(\mathbf{r}) = n_o(\mathbf{r}) \nu_i(\mathbf{r}) \quad (5)$$

In the last definition, ν_i is the number of newly created ions per time unit, or equally the number of photoionized or charge-exchanged oxygen atoms per time unit.

Assuming that plasma picks up the new ions instantly, ionized atoms acquire immediately the velocity and the temperature of the solar wind. In these conditions, the number density of ions obeys the continuity equation:

$$\text{div} (n_{o^+}(\mathbf{r}) \mathbf{v}_p(\mathbf{r})) = q_1(\mathbf{r}) \quad (6)$$

The boundary condition for the distribution function $f_o(\mathbf{r}, \mathbf{w}_o)$ is the Maxwell distribution:

$$f_{o,\infty}(\mathbf{w}_o) = \left(\frac{1}{c_o \sqrt{\pi}} \right)^3 \exp \left(- \frac{(\mathbf{w}_o - \mathbf{v}_\infty)^2}{c_o^2} \right) \quad (7)$$

(where $c_o = (\frac{2kT_{O,\infty}}{m_o})^{1/2}$).

The number density of oxygen ions at the outer boundary is determined by the ionization balance which prevails in the unperturbed medium:

$$\frac{n_{o^+}}{n_o} = \frac{8}{9} \frac{n_{H^+}}{n_H} \text{ (Stebbins et al., 1964).}$$

4. Method of calculation

The previous set of equations shows that the numbers of direct and reverse charge-exchange processes are of the same order, and that, due to the reverse charge-exchange, the calculation of the oxygen atoms distribution depends on the oxygen ions distribution. As a consequence, both distributions have to be evaluated self-consistently.

To do so, in replacement of the two integro-differential Eqs. (1) and (2), we use an iterative method to solve alternatively the four terms of equation system (3) on the one hand (step 1) and the continuity equation for O ions (4) on the other (step2). More specifically, being given an initial oxygen ions distribution, the number density, the velocity and the temperature of the oxygen atoms as well as the mass source for oxygen ions (Eq. (4)) are calculated with a Monte-Carlo method with trajectory splitting, simulating the flow of a Maxwellian population of O atoms through an interface where it interacts with protons, photons and gravity. Then the resulting ions source is used to calculate numerically the new ion density distribution n_{o^+} (step 2), which is reinjected in the next Monte-Carlo computation, etc... The process is stopped when both distributions have converged.

The number density of oxygen ions at the inner boundary is not preliminarily fixed and is here a result of the calculation. Numerical experiments with Eq. (4) show that this parameter has a non-negligible influence in only a very small region near the Sun.

The Monte-Carlo method with splitted trajectories used here is similar to the one build by Malama (1991) for the heliospheric interface neutral H - proton coupling. The computational region, shown in Fig. 1, is divided into cells defined by 50 radial distances and 40 angles. Oxygen and hydrogen atom fluxes at the external boundary surface are characterized by maxwellian distribution for the same temperature and bulk velocity as the neutral H and the protons. More specifically, for each velocity vector \mathbf{w} making an angle θ with the normal to the boundary surface, the infinitesimal flux out from the surface corresponding to this velocity vector is identical to the infinitesimal flux corresponding to a maxwellian distribution entering the surface.

$$f_{A,\infty}(\mathbf{r}, \mathbf{w}_A) = \frac{(\mathbf{w}_A, \mathbf{l}) f_{A,\infty}^{maxwell}(\mathbf{w}_A)}{\int \int (\mathbf{w}_A, \mathbf{l}) f_{A,\infty}^{maxwell}(\mathbf{w}_A) d\mathbf{w}_A d\theta}$$

where \mathbf{l} is the inner normal to the boundary surface, $f_{A,\infty}^{maxwell}(\mathbf{w}_A)$ is the Maxwell distribution function of the A-atoms in the unperturbed LISM. A equals O for O atoms and H for H atoms.

During the Monte-Carlo simulation, each O or H atom is followed along its trajectory, which is influenced by gravity (for O atom) or gravity plus radiation pressure (for H atom). If it is photoionized, this atom disappears from the calculation and, for O, a new oxygen ion is created. For O, when it experiences a charge exchange with a proton, a new oxygen ion is created and the O atom disappears from the calculation. For H, when it experiences a charge exchange with an oxygen ion, a new

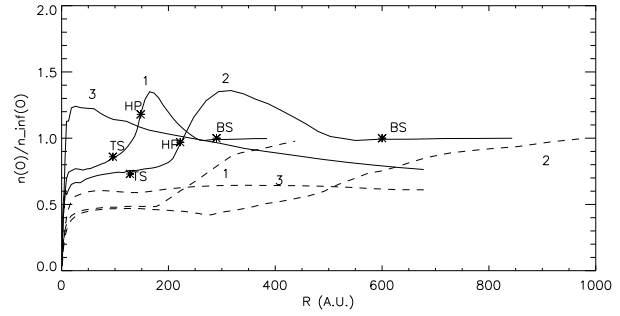


Fig. 3. Number density of oxygen LISM atoms in units of the unperturbed LISM density, as a function of the heliocentric distance. Curves 1,2,3 are for upwind, sidewind and downwind respectively. n_{∞}^O is the oxygen atom number density in the unperturbed LISM. Positions of TS, HP and BS are shown by stars.

oxygen atom is created, with a velocity selected in the distribution of the local plasma, and its trajectory is computed again. For an H atom, when it experiences a charge exchange with a proton, a new H atom is created, with a velocity selected in the distribution of the local plasma, and its trajectory is computed again. The H atoms are necessary to obtain the inner sources of O atoms, which are mainly due to charge exchange of H atoms with O ions. For the H atoms-protons charge-exchange the following parameters are used:

$\sigma_{ex}^{HH^+} = (a_1 - a_2 \lg(u))^2$, cm^2 is the charge exchange cross section, with $u = |\mathbf{w}_p - \mathbf{w}_H|$ being the relative atom-proton velocity measured in centimeters per second, a_1, a_2 are constants, $a_1 = 1.64 \times 10^{-7}$, $a_2 = 1.6 \times 10^{-8}$ (Maher & Tinsley, 1977). The photoionization rate on the Earth's orbit equals $\beta_{pe}^H = 8.8 \times 10^{-8} \text{sec}^{-1}$ (Banks, Kockarts, 1973). The ratio of Ly_{α} radiation pressure to gravitation is here equal to 0.55. For a good statistical accuracy, splitting procedures are used (Malama, 1991). Density and sources of O atoms are calculated within each cell of a grid.

5. Numerical results

The simulation was performed for a number density of oxygen in the unperturbed interstellar medium $n_{o,\infty}^{LISM}$ equal to $0.1 \times 10^{-3} \text{cm}^{-3}$. This corresponds to a ratio of oxygen to hydrogen number densities $\frac{n_{O,\infty}}{n_{H,\infty}}$ of $7.1 \cdot 10^{-3}$. This is close to the most recent neutral oxygen/neutral hydrogen relative abundance measurements in the Local Interstellar Cloud (or LIC) of Linsky et al (1993) (see Sect. 6). Since the influence of the oxygen distribution on the protons and neutral H atoms is negligible, the densities resulting from the present calculations are simply scaled by the chosen neutral oxygen density (and the corresponding oxygen ions density). In other words, in case of a different O/H abundance ratio, oxygen atoms and ions density distributions can be obtained from the present results by simply multiplying by the appropriate constant. However, this is no longer the case of H, since ionizations of O and H in the unperturbed LISM are entirely coupled. In this case, new computations are required.

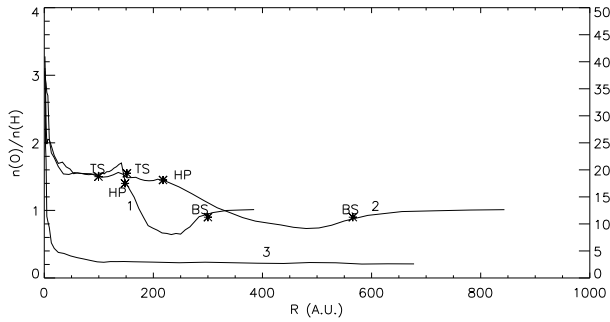


Fig. 4. Ratio of the neutral oxygen to the neutral hydrogen density as function of heliocentric distance for the upwind direction (1), the sidewind or perpendicular direction (2) and the downwind direction (3). The ratio is in units of the ratio in the unperturbed LISM. Curve 3 corresponds to the right scale. On the downwind side the oxygen to hydrogen ratio reaches values as high as 40 due to the combined effects of oxygen focusing and hydrogen depletion, and remains larger than one even at very large distances from the Sun, because the hydrogen density remains below the interstellar level (see Fig. 3a). The positions of TS, HP and BS are indicated.

Fig. 3 shows the resulting density of oxygen atoms as a function of the heliocentric distance, as it comes out of the iterative process. Dashed curves correspond to the hypothetical case $n_{H,\infty} = 0 \text{ cm}^{-3}$ in the unperturbed LISM (case a), while the solid curves are for $n_{H,\infty} = 0.14 \text{ cm}^{-3}$ (case b). In case a) only direct charge exchange is taken into account, because there are no H atoms in the unperturbed LISM. In case b) both direct and reverse charge exchange are taken into account. Fig. 3 shows that the region between the bow shock and the terminal shock acts as a kind of filter for the interstellar oxygen, with a larger transmission on the downwind side as compared with the opposite direction. As a matter of fact, oxygen densities are smaller than one inside the termination shock on the upwind and sidewind directions, and close to one on the downwind side. Closer to the Sun, inside about 10 A.U., the solar gravitation and the photoionization become the essential processes acting on O atoms, creating the ionization cavity and the downwind focusing cone. Close to the Sun on the downwind side ionization and gravitation act in opposite ways: the gravitation increases the number density of atoms near the Sun, while the photoionization decreases it. The gravitational focusing is responsible for high downwind densities only if the ionization is not too strong. The curve 3, which corresponds to the downwind direction, shows the density increase due to the gravitation (the focusing effect).

Fig. 3 also clearly shows a density rise in the region between the outer shock and the heliopause, most pronounced in the upwind direction. The comparison of the solid and dashed curves shows that this density increase (or “oxygen wall”) is entirely the consequence of the reverse charge exchange between hydrogen atoms and oxygen ions. This effect becomes very small at large angles from the upwind direction. A similar compression was derived for the first time for the neutral hydrogen by Baranov and Malama (1993) (Fig 2d). The “hydrogen wall” is due to secondary H atoms newly born after charge-exchange with

the protons of the decelerated, compressed and heated plasma. While the maximum compression ratio reaches 1.6-1.7 for the H wall (Fig 2d), it reaches an almost equivalent level (1.3-1.4) in the oxygen wall, despite the significantly smaller charge-exchange cross-section.

The comparison between solid and dashed curves also shows that the reverse charge-exchange has as a result to fill the whole heliosphere, but the filling is done preferentially on the downwind side, for regions closer to the Sun than about 100 A.U. The gravitational focusing is responsible for these high downwind densities.

In Fig. 4 is represented the ratio of oxygen to hydrogen atom number densities as a function of heliocentric distance. This ratio has a complex behavior around the interface and increases inside the heliosphere, especially on the downwind side. The differences between the O and H filling of the downwind cavity are related to the differences between oxygen and hydrogen masses. While the bulk velocities of oxygen and hydrogen are the same, the thermal velocities depend on the number larger by a factor of four for oxygen as compared with hydrogen, and then in a larger filling of the downwind cavity. Note that the results of the simulation for the cells closer than 30 A.U. from the Sun on the upwind side are not very precise, because the Monte-Carlo algorithm used here provides poorer statistics in this region.

Fig. 5 shows the distribution of the oxygen ion source derived from the charge exchange processes and the photoionization. This distribution may be used as an input in models which describe how new born ions are picked up by solar wind. There is strong increase of the source at decreasing distance from the Sun. The reason for this increase is mainly the photoionization. Between the bow shock and the heliopause and between the heliopause and the terminal shock the

The volumic density of oxygen ions obtained by assuming the simplest ion pick up model, i.e. immediate assimilation of the ions by the ambient plasma, is displayed on Fig. 6, normalized to the value of O^+ at infinity. It is clear that the resulting distribution is similar to the proton distribution (fig.2a), while by definition the velocity and temperature of the oxygen ions are identical to those of protons (fig. 2b, Fig. 2c). These model results can be used for the of pick-up ions (Geiss et al, 1994).

6. Comparisons with observations and inferences on the LIC electron density

One of the main results of the present model is the very small rejection of neutral oxygen outside the heliosphere. As a matter of fact, for the relatively high plasma density used for the computation, about 70% of the neutral O succeeds in penetrating closer than 50 A.U. from the Sun on the upwind side. For a given number density ratio between the heliosphere and the ISM, such an easy entrance allows for higher interstellar plasma densities.

At present the most accurate comparison between interstellar and heliospheric oxygen makes use of Hubble Space Telescope (HST) nearby stars observations on the one hand, and

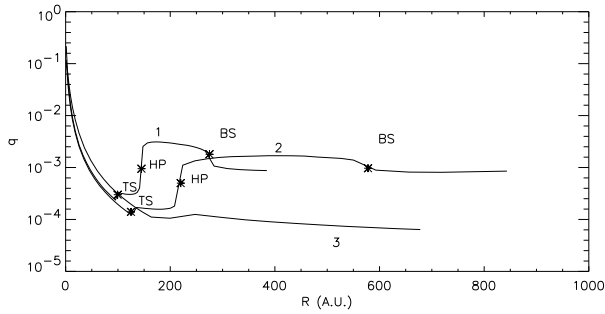


Fig. 5. Sources of oxygen LISM's ions as function of heliocentric distance for upwind direction (1), perpendicular direction (2) and downwind direction (3). The sources are in units of $\frac{\rho_{O,\infty} V_{LISM,\infty}}{\tau_E}$. Positions of TS, HP and BS are shown points

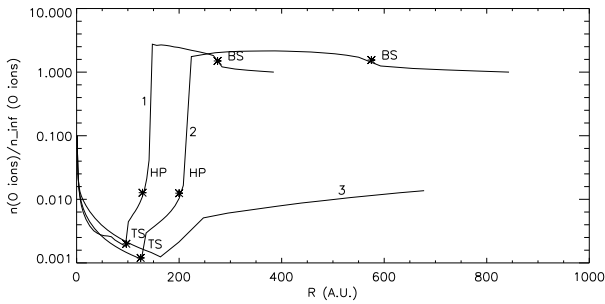


Fig. 6. Number density of oxygen pick-up ions normalized to the density of oxygen ions in the unperturbed LISM.

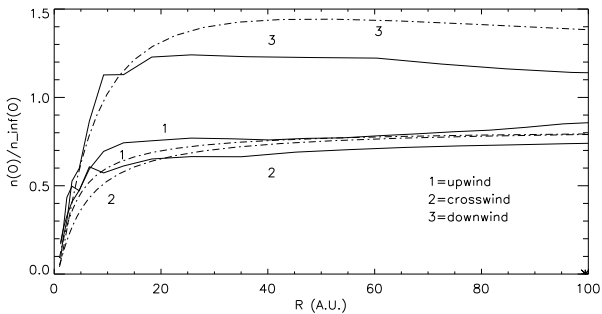


Fig. 7. Number density of oxygen atoms normalized to the density in the unperturbed ISM with (solid lines) and without (dot-dashed lines) interface perturbations for the same interstellar and solar parameters. Densities have been divided by 1.2 for the classical model without interface.

Ulysses SWICS O^+ pick-up data on the other. The most appropriate HST data in the solar environment are those of Linsky et al (1993). These authors have measured both neutral oxygen and neutral hydrogen columns along the line-of-sight towards the nearby star Capella. Towards this target located at 12 pc, only one velocity cloud component produces interstellar absorption lines, the one corresponding to our Local Cloud (Lallement and Bertin, 1992, Lallement et al, 1995). As a consequence, relative abundances deduced from column-densities calculations towards this star directly apply to the LIC (and not to companion clouds) and are the most representative of the extra-heliospheric

gas. The Linsky et al data imply a neutral oxygen to neutral hydrogen ratio OI/HI of $4.8 \cdot 10^{-4}$ with a rather small uncertainty of the order of 10%. From the charge-exchange equilibrium described in Sect. 3, the corresponding O ions density outside of the heliosphere is $4.2 \cdot 10^{-4} n_e \text{ cm}^{-3}$, and is independent of the neutral H density. For a plasma density of 0.1 cm^{-3} , and using the Fig. 6, the ion density at 5 A.U. is found to be $0.015 \times 4.2 \cdot 10^{-5} = 6.4 \cdot 10^{-7} \text{ cm}^{-3}$. The corresponding ion flux assuming all ions are moving at the solar wind speed chosen for the model (450 km s^{-1}) is found to be of the order of $30 \text{ ions cm}^2 \text{ s}^{-1}$. This number is dependent on our assumptions on the local proton (= electron) and neutral H densities and on the (assumed constant) solar wind characteristics.

The oxygen ions flux detected by the SWICS instrument at 5 A.U. was of the order of $3100 \cdot 6 \cdot 10^{-3} = 19 \cdot \text{cm}^2 \text{ s}^{-1}$ (Geiss et al, 1994 and Gloeckler et al, 1993).

The theoretical and measured values then agree within a factor of 1.5. If taken strictly, the SWICS measurements imply a larger filtration and a plasma density higher than the model value used here, i.e. 0.1 cm^{-3} , or alternately a smaller oxygen density. However a smaller oxygen density implies a smaller neutral H density, and the value we have used here is very close to the lower limit for the neutral hydrogen outside the heliosphere (see Quémerais & al, 1994.) However, in our opinion, the model assumptions on the one hand, in particular the absence of magnetic field, and the constancy of the solar wind, the uncertainties in the fluxes measurements on the other hand (e.g. ions at velocities of the order of 800 km s^{-1} are not detected, and the ion flux close to the Sun is directly related to the instantaneous solar wind), preclude such a firm conclusion. More data are needed for averaging over spatial and temporal variations of the solar wind and the photoionization. Nevertheless, this rough agreement is promising. It also certainly shows that there is not too much oxygen in the heliosphere for precluding a filtering. On the contrary, the comparison with the interstellar data suggests a substantial filtering, possibly an already decrease included in the present model, plus the suggested additional decrease by 1.5 quoted above).

The neutral oxygen abundance relatively to helium has been deduced by Geiss et al (1994) from oxygen ions fluxes by comparison with pick-up helium fluxes, in the context of classical models, i.e. the resulting number refers to the inner heliosphere, outside the region of significant interaction with the Sun. A He/O ratio of 290 (+ 190, -100) has been inferred from zero temperature models for O and He. Although the comparison is more indirect than the previous one, it is in with the astronomical observations of Linsky et al (1993), which provide $HI/OI=2,100$. However, it requires an assumption about the HI/HeI ratio. The Extreme UltraViolet Explorer measurements have provided a series of determination of this ratio towards nearby white dwarfs, with the conclusion that HI/HeI is comprised in the range 9.3- 20.0 depending on the targets, with a mean value of 14.5, implying that in the Sun environment helium is always at least as ionized as hydrogen (Dupuis et al, 1995). We will make use of these results. If the helium and hydrogen were equally ionized ($HI/HeI = 10$, i.e. close to the lower value) then

the Linsky LIC results give $\text{HeI/OI} = 210$. If HI/HeI has the mean value 14.5 then the Linsky data imply $\text{HeI/OI} = 145$. If one compares with the total range of values derived by Geiss & al (190-480), this implies a large range of possibilities, including no filtration on one hand, or a very strong decrease by a factor of 3 on the other. As a conclusion, the oxygen/helium ratio is also compatible with filtration of the oxygen atoms. However, the Geiss & al (1994) O and He ions relative fluxes are in good agreement with their models if the oxygen ionization rate is of the order of $3 \cdot 10^{-7} \text{ s}^{-1}$ or less. This is in one sense satisfying because it is a reasonable value. But, as already noticed by Fahr & al, 1995, the use of such a reasonable ionization rate, results in a very high HeI/OI ratio of about 400 or more, much larger than the solar system value of 114 suggesting a very strong filtration.

Here we compare with what has been shown above to be the most likely interstellar ratio ($\text{HeI/OI} = 145\text{-}210$), i.e. a more appropriate quantity, somewhat larger than the solar system value, but it still implies a rather strong filtration (a decrease by a factor of at least 2). A filtration as large as by a factor of 2 is certainly precluded because it would imply a too large plasma density and then a too small heliosphere. Further work is needed to explain these contradictions, in terms of differences between classical and interface models, or the neglect of one or more processes. A first attempt here is a comparison between the distribution of O atoms at small heliocentric distances as it comes out from the interface model, with a density distribution issued from classical hot models without interface (only supersonic solar wind).

In Fig. 7 are plotted oxygen densities calculated in the frame of a "classical" model for the same velocity and temperature of the inflowing oxygen as those prevailing outside the heliosphere in the interface model. In the classical case the photo-ionization and the charge-exchange are represented by a unique term for loss processes calculated for the mean solar wind velocity, and varying as r^{-2} . This is at variance with the full model for which all charge-exchange velocity of the ion and the atom. The total ionization rate at 1 A.U. is $5.79 \cdot 10^{-7} \text{ s}^{-1}$ (lifetime against ionization $1.73 \cdot 10^6 \text{ s}$). The comparison is done for upwind, sidewind and downwind lines-of-sight. To allow an easier comparison, classical densities have been divided by 1.2, which corresponds to the filtration factor on the upwind side. Although our statistics are too poor to quantify in a precise way the changes in the filling very close to the Sun, the densities issued from the two models are not extremely different, except at large distances (the oxygen wall) and possibly very close to the Sun, and no firm conclusions can be derived from this first attempt.

We now turn our attention to the cosmic ray measurements. The ACR are observed in the outer heliosphere by the Voyager cosmic ray instruments since 1977. In addition to oxygen, He, Ne, C, N and Ar are also detected, allowing for the first time relative abundances determinations of neutral species in the interstellar extra-heliospheric gas, through modelling of the ionization, pick-up and acceleration processes (e.g. Cummings et al, 1984, Jokipii, 1986, Cummings and Stone, 1990). It was recently suggested by Frisch (1994) to make use of the C and O abundances derived from the ACR, to infer the electron density in the local ISM. When applying this method, Frisch

(1994,1995) deduces an electron density range of $0.22\text{-}0.63 \text{ cm}^{-3}$, largely above previous estimates, but in good agreement with independent estimates from the interstellar magnesium equilibrium, as observed from the absorption lines in stellar spectra (Lallement et al, 1995), also providing a surprisingly large electron density. In principle, these estimates from ACR data should include a correction for the neutral oxygen filtration, because only pick-up ions created in the supersonic solar wind have a peculiar enough velocity distribution making them the seed particles in the ACR production. A very precise correcting factor requires a full analysis combining ACR convection models and O-ion source functions as presented here, which is well beyond the scope of this work. However, a simple look at Fig. 3, 5 and 6 shows that for the two-shocks model for $n_e = 0.1 \text{ cm}^{-3}$, the total number of neutral oxygen atoms which penetrates the supersonic wind region, is smaller by at most 30% as compared with the "no interface" case. As a consequence, on this basis it does not appear necessary to apply a large correction to the Frisch (1994) results. A rough estimate shows that the inferred plasma density decreases by about the same amount. It remains that carbon filtration also be computed, which is a difficult task due to uncertainties in the charge-exchange cross-sections.

7. Conclusions

On the basis of the above simulations we can draw the following conclusions:

1. Interstellar oxygen atoms do penetrate the heliosphere and the Solar system while significantly interacting with the plasma component. The degree of penetration, is found to be of the same order, although larger than the neutral hydrogen filtration. It is due to the charge-exchange cross sections being of the same order for these elements. However, the comparison between models with zero and substantial neutral H density in the unperturbed LISM shows a very strong influence of the O ion - H atom charge exchange (the reverse charge-exchange) on the oxygen atom distribution. As a result, the inner heliosphere is filled with a very large fraction of secondary atoms resulting from the this reverse charge-exchange. This has as a consequence to favor oxygen entrance in the heliosphere.

The fraction of neutral oxygen penetrating the heliosphere is rather high, of about 70% on the upwind side for an interstellar plasma density of 0.1 cm^{-3} (or about 20 to 30% losses).

2. One of the features coming out from the present two shocks model is the presence of an oxygen atom density maximum in the region between the bow shock and the heliopause (an "oxygen-wall"), with a density value higher than the density at infinity. This effect was already discovered for neutral hydrogen (Baranov and Malama, 1993). It is mainly due here to the reverse charge-exchange between compressed neutral H and O ions. However, it is less pronounced than the neutral H "wall".

4. A spectacular result of these simulations is the increase of the oxygen to hydrogen density ratio near the Sun and on the downwind side, which is mainly due to the differences between the oxygen and hydrogen masses. This effect is already

present close to the Sun in the absence of heliospheric interface perturbations.

5. Recent nearby stars spectroscopic observations with the HST have provided the neutral oxygen to neutral hydrogen ratio in the Local Cloud (data from Linsky & al (1993)), allowing an estimate of the oxygen ions fluxes in the Sun vicinity in the frame of the present model. The comparison with the Ulysses measurements (Gloeckler & al, 1993) favours oxygen losses of the order of 50% (about 30% more than predicted by the present model), and subsequently interstellar plasma densities larger than 0.1 cm^{-3} . When compared with the most recent interstellar abundances measurements, the helium to oxygen ratio derived from the Ulysses observations (Geiss & al, 1994) also implies a significant depletion of oxygen in the inner heliosphere (by a factor of at least 2), if one considers the most probable range for the ionization rate, and the best fit to the data. However, further modeling is required, with, in particular, the inclusion of electron impact ionization processes, and improved statistics close to the Sun.

Acknowledgements. We would especially like to thank Prof. V.B. Baranov for having stimulated this research and for useful discussions. Many thanks also to Dr. S.V. Chalov for the fruitful discussions we had with him. We acknowledge the support of the International Science Foundation and the Russian Government under contract N J2E100 and by the Russian Foundation of Fundamental Investigations under contract N 95-02-042-15. We thank our referee D. Rucinski for his very careful and competent analysis of the paper, which led to the detection of an error in the comparison with the classical model, and his numerous useful comments.

References

- Axford W.I., 1989, in *Physics of the Outer Heliosphere*, Cospar Coll. Series (1) 7, Pergamon
- Banks P.M., Kockarts, Aeronomy, 1973
- Baranov, V.B., Krasnobaev, K.V. and Kulikovskiy, A.G., 1971, *Soviet Phys. Doklady*, 15, 791
- Baranov V.B. and M.S. Ruderman, 1979, *Pisma Astron.Zh.*, 5, 615-619
- Baranov V.B., 1990, *Space Sci. Rev.*, 52, 89
- Baranov, V.B., Lebedev, M.G., Malama, Yu.G., 1991, *Astroph. J.* 375, 347-351
- Baranov, V.B. and Malama, Yu.G., 1993, *J. Geophys. Res.* 98 (9), 157
- Bleszynski, S. 1987, *A&A* 180, 201
- Bowyer, S. and Fahr, H.J., 1989, In *Proc. of COSPAR Symposium on Physics of the outer heliosphere*, Warsaw (Poland), Sept. 1989, 29-36
- Cummings A.C., Stone E.C., Webber W.R., 1984, *ApJ*, 287, L99
- Cummings A.C., Stone E.C., 1990, 21 st Int. Cosmic Ray Conf. 6, 202
- Cummings A.C., Stone E.C., Webber W.R., 1993, *JGR* 98, A9, 15165
- Dupuis J., Vennes S., Bowyer S., 1995, *ApJ*, 455, 574
- Fahr, H.J. and Ripken, H.W., 1984, *A&A* 139, 551
- Fahr, H.J. 1989, In *Proc. of COSPAR Symposium on Physics of the outer heliosphere*, Warsaw (Poland), Sept. 1989, 327-343
- Fahr, H.J., 1991, *A&A* 241, 251
- Fahr, H.J., Osterbart, O. and Rucinski, D. 1995, *A & A*, 294, N 2, 584
- Fisk, L.A., Kozlovsky, B. and Ramaty, R. 1974, *Ap. J. Lett.*, 190, L35
- Frisch P.C., 1994, *Science*, 265, 1423
- Frisch P.C., 1995, *Space Science Reviews*, 72, 499
- Gangopadhyay, P. and Judge, D.L., 1989, *Ap. J.* 336, 999

- Geiss J., Gloeckler G., Mall U., von Steiger R., Galvin A.B., Ogilvie K.W., 1994, *A&A* 282, 924
- Gloeckler G., Geiss J., Balsiger H., Fisk L.A., Galwin A.B., Ipavich F.M., Ogilvie K.W., von Steiger R., Wilken B., 1993, *Science*, 261, 70
- Gloeckler G., Fisk L.A., Schwadron N., Geiss J., 1995, *Geophys. Res. Lett.*, 22, 2665
- Holzer, T.E., 1989, *Ann. Rev. of Astronomy and Astrophysics*, 27, 199
- Jokipii, J.R. 1971, *Rev. Geophys. Space Res.*, 9, 27 1971
- Jokipii, J.R., McDonald, 1995 *Scientific American*, 272 (4), 58
- Jokipii, J.R., *J. Geophys. Res.*, 91, 2929, 1986
- Kurth W.S., Gurnett D.A., 1993, *JGR* 98 (A9), 15129
- Lallement R., Bertin P., 1992, *A&A* 266, 479
- Lallement R., Bertaux J.L., Clarke J.T., 1993, *Science*, 260, 1095
- Lallement R., Ferlet R., Lagrange A.M., Lemoine M., Vidal-Madjar A., 1995, *A&A*, 304 (2), 461
- Lee M., 1993, *Adv. Space Res.* 13, (6) 283
- Linsky J.L., Brown A., Gayley K. 1993, *Ap.J.* 402, 694
- Maher L.J., Tinsley B.A., 1977, *J. Geophys. Res.* 82-4, 689
- Malama, Yu.G. 1991, *Ap&SS* 176, 21
- Mobius E.D., Klecker B., Hovestadt D., Scholer M., 1988, *Ap&SS.* 144, 487
- Osterbart R., Fahr, H.J. 1992, *A&A* 264, 260
- Parker, E.N., 1961, *Astrophys. J.* 134, 20-27
- Pesses M.E., Jokipii J.R., Eichler D., 1981, *ApJ*, 246, L85
- Qu  merais E., Bertaux J.L., Sandel B.R., Lallement R., 1994, *A&A*, 290, 941
- Ripken H.W. and Fahr H.J., 1983, *A&A* 122, 181
- Stebbing, R.F., Smith, A.C.H., Ehrhardt, H., 1964, *J. Geophys. Res.*, 69, 2349
- Suess S.T., 1990, *Rev. Geophys.* 28, 97
- Wallis, M.K. 1975, *Nature*, 254, 207
- Witte M., Rosenbauer H., Banaszkiewicz M., Fahr H.J., 1993, *Adv. Space Res.* 13,(6) 121